Multi-section fission ionization chamber for measurement of 239 (,) reaction in fission tagging method

(n_TOF Collaboration) Perkowski, J.; Alcayne, V.; Andrzejewski, J.; Cano-Ott, D.; Gawlik-Ramięga, A.; Mendoza, E.; Sánchez-Caballero, A.; Sibbens, G.; Vanleeuw, D.; Aberle, O.; ...

Source / Izvornik: **Nuclear Instruments and Methods in Physics Research Section A: Accelerators, Spectrometers, Detectors and Associated Equipment, 2024, 1067**

Journal article, Published version
Rad u časopisu, Objavljena verzija rada (izdavačev PDF)

https://doi.org/10.1016/j.nima.2024.169649

Permanent link / Trajna poveznica: https://urn.nsk.hr/urn:nbn:hr:217:108064

Nuclear Instruments and Methods in Physics Research A 1067 (2024) 169649

Contents lists available at ScienceDirect

Nuclear Inst. and Methods in Physics Research, A

journal homepage: www.elsevier.com/locate/nima

Full Length Article

Multi-section fission ionization chamber for measurement of $^{239}Pu(n,\gamma)$ reaction in fission tagging method

J. Perkowski [1,*], V. Alcayne [2], J. Andrzejewski [1], D. Cano-Ott [2], A. Gawlik-Ramięga [1], E. Mendoza [2], A. Sánchez-Caballero [2], G. Sibbens [3], D. Vanleeuw [3], O. Aberle [4], S. Altieri [5,6], S. Amaducci [7], V. Babiano-Suarez [8], M. Bacak [4], J. Balibrea Correa [8], C. Beltrami [5], S. Bennett [9], A.P. Bernardes [4], E. Berthoumieux [10], R. Beyer [11], M. Boromiza [12], D. Bosnar [13], M. Caamaño [14], F. Calviño [15], M. Calviani [4], A. Casanovas [15], D.M. Castelluccio [16,17], F. Cerutti [4], G. Cescutti [18,19], S. Chasapoglou [20], E. Chiaveri [4,9], P. Colombetti [21,22], N. Colonna [23], P. Console Camprini [17,16], G. Cortés [15], M.A. Cortés-Giraldo [24], L. Cosentino [7], S. Cristallo [25,26], S. Dellmann [27], M. Di Castro [4], S. Di Maria [28], M. Diakaki [20], M. Dietz [29], C. Domingo-Pardo [8], R. Dressler [30], E. Dupont [10], I. Durán [14], Z. Eleme [31], S. Fargier [4], B. Fernández [24], B. Fernández-Domínguez [14], P. Finocchiaro [7], S. Fiore [16,32], V. Furman [33], F. García-Infantes [34,4], G. Gervino [21,22], S. Gilardoni [4], E. González-Romero [2], C. Guerrero [24], F. Gunsing [10], C. Gustavino [32], J. Heyse [3], W. Hillman [9], D.G. Jenkins [35], E. Jericha [36], A. Junghans [11], Y. Kadi [4], K. Kaperoni [20], G. Kaur [10], A. Kimura [36], I. Knapová [37], M. Kokkoris [20], Y. Kopatch [33], M. Krtička [37], N. Kyritsis [20], I. Ladarescu [8], C. Lederer-Woods [38], J. Lerendegui-Marco [8], G. Lerner [4], A. Manna [17,39], T. Martínez [2], A. Masi [4], C. Massimi [17,39], P. Mastinu [40], M. Mastromarco [23,41], E.A. Maugeri [30], A. Mazzone [23,42], A. Mengoni [16,17], V. Michalopoulou [20], P.M. Milazzo [18], R. Mucciola [25,43], F. Murtas [44], E. Musacchio-Gonzalez [40], A. Musumarra [45,46], A. Negret [12], A. Pérez de Rada Fiol [2], P. Pérez-Maroto [24], N. Patronis [31,4], J.A. Pavón-Rodríguez [24,4], M.G. Pellegriti [45], C. Petrone [12], E. Pirovano [29], J. Plaza del Olmo [2], S. Pomp [47], I. Porras [34], J. Praena [34], J.M. Quesada [24], R. Reifarth [27], D. Rochman [30], Y. Romanets [28], C. Rubbia [4], M. Sabaté-Gilarte [4], P. Schillebeeckx [3], D. Schumann [30], A. Sekhar [9], A.G. Smith [9], N.V. Sosnin [38], M.E. Stamati [31,4], A. Sturniolo [21], G. Tagliente [23], A. Tarifeño-Saldivia [15], D. Tarrío [47], P. Torres-Sánchez [34], E. Vagena [31], S. Valenta [37], V. Variale [23], P. Vaz [28], G. Vecchio [7], D. Vescovi [27], V. Vlachoudis [4], R. Vlastou [20], A. Wallner [11], P.J. Woods [38], T. Wright [9], R. Zarrella [17,39], P. Žugec [13]

[1] *University of Lodz, Poland*
[2] *Centro de Investigaciones Energéticas Medioambientales y Tecnológicas (CIEMAT), Spain*
[3] *European Commission, Joint Research Centre (JRC), Geel, Belgium*
[4] *European Organization for Nuclear Research (CERN), Switzerland*
[5] *Istituto Nazionale di Fisica Nucleare, Sezione di Pavia, Italy*
[6] *Department of Physics, University of Pavia, Italy*
[7] *INFN Laboratori Nazionali del Sud, Catania, Italy*
[8] *Instituto de Física Corpuscular, CSIC - Universidad de Valencia, Spain*
[9] *University of Manchester, United Kingdom*
[10] *CEA Irfu, Université Paris-Saclay, F-91191 Gif-sur-Yvette, France*
[11] *Helmholtz-Zentrum Dresden-Rossendorf, Germany*
[12] *Horia Hulubei National Institute of Physics and Nuclear Engineering, Romania*
[13] *Department of Physics, Faculty of Science, University of Zagreb, Zagreb, Croatia*
[14] *University of Santiago de Compostela, Spain*
[15] *Universitat Politècnica de Catalunya, Spain*

* Corresponding author.
E-mail address: jaroslaw.perkowski@uni.lodz.pl (J. Perkowski).

https://doi.org/10.1016/j.nima.2024.169649
Received 9 May 2024; Received in revised form 10 July 2024; Accepted 20 July 2024
Available online 25 July 2024

[16] Agenzia nazionale per le nuove tecnologie (ENEA), Italy
[17] Istituto Nazionale di Fisica Nucleare, Sezione di Bologna, Italy
[18] Istituto Nazionale di Fisica Nucleare, Sezione di Trieste, Italy
[19] Department of Physics, University of Trieste, Italy
[20] National Technical University of Athens, Greece
[21] Istituto Nazionale di Fisica Nucleare, Sezione di Torino, Italy
[22] Department of Physics, University of Torino, Italy
[23] Istituto Nazionale di Fisica Nucleare, Sezione di Bari, Italy
[24] Universidad de Sevilla, Spain
[25] Istituto Nazionale di Fisica Nucleare, Sezione di Perugia, Italy
[26] Istituto Nazionale di Astrofisica - Osservatorio Astronomico di Teramo, Italy
[27] Goethe University Frankfurt, Germany
[28] Instituto Superior Técnico, Lisbon, Portugal
[29] Physikalisch-Technische Bundesanstalt (PTB), Bundesallee 100, 38116 Braunschweig, Germany
[30] Paul Scherrer Institut (PSI), Villigen, Switzerland
[31] University of Ioannina, Greece
[32] Istituto Nazionale di Fisica Nucleare, Sezione di Roma1, Roma, Italy
[33] Affiliated with an institute covered by a cooperation agreement with CERN
[34] University of Granada, Spain
[35] TU Wien, Atominstitut, Stadionallee 2, 1020 Wien, Austria
[36] Japan Atomic Energy Agency (JAEA), Tokai-Mura, Japan
[37] Charles University, Prague, Czech Republic
[38] School of Physics and Astronomy, University of Edinburgh, United Kingdom
[39] Dipartimento di Fisica e Astronomia, Università di Bologna, Italy
[40] INFN Laboratori Nazionali di Legnaro, Italy
[41] Dipartimento Interateneo di Fisica, Università degli Studi di Bari, Italy
[42] Consiglio Nazionale delle Ricerche, Bari, Italy
[43] Dipartimento di Fisica e Geologia, Università di Perugia, Italy
[44] INFN Laboratori Nazionali di Frascati, Italy
[45] Istituto Nazionale di Fisica Nucleare, Sezione di Catania, Italy
[46] Department of Physics and Astronomy, University of Catania, Italy
[47] Department of Physics and Astronomy, Uppsala University, Box 516, 75120 Uppsala, Sweden

ARTICLE INFO

Keywords:
Radiative neutron capture cross section
Fission
Ionization chamber
^{239}Pu
n_TOF facility
CERN

ABSTRACT

The $^{239}Pu(n,\gamma)$ reaction cross section is very important for operation of both thermal and fast reactors, when loaded with MOX fuels. According to the NEA/OECD High Priority Request List the precision of cross section data for this reaction should be improved. The cross section of (n,f) reaction is much higher compared to (n,γ) for this isotope. In such conditions the fission tagging technique could be applied to identify the fission background. In the past, this technique was successfully used for capture measurements at the n_TOF facility at CERN. The multi-section fission ionization chamber was constructed and used in the combination with Total Absorption Calorimeter (TAC) for detecting gamma rays for the precise measurement of $^{239}Pu(n,\gamma)$ reaction cross section at the n_TOF facility.

1. Introduction

The reduction of uncertainties in the radiative neutron capture cross section measurements of fissile isotopes plays an essential role for safer and more economic design of modern nuclear systems such as Gen-IV reactors and Accelerator Driven Systems [1,2]. However, these measurements are challenging due to the disadvantageous competition between the (n,γ) cascades and prompt fission γ-rays.

As was mentioned at the beginning, ^{239}Pu plays a dominant role in the reactor industry. Existing experimental data from EXFOR [3] are not consistent. Hence, more accurate ^{239}Pu capture and fission cross section data are needed [4,5]. For that reason, the ^{239}Pu(n,γ) reaction cross section has been listed in the NEA/OECD High Priority Request List, where authors claim that these data should be improved in neutron energy range 1 meV ÷ 1.35 MeV [6]. However for this isotope, cross section of (n,f) reaction is much higher compared to (n,γ) up to 10 eV, and similar for higher energies, what is shown in Fig. 1. To identify significant background contribution due to the fission, the fission tagging technique can be used. It has been previously successfully applied at the n_TOF facility at CERN. Namely, the measurement of ^{235}U(n,γ) and ^{235}U(n,f) cross sections were determined using the simultaneous use of Total Absorption Calorimeter (TAC) [7–9] and MicroMegas fission detector [10] or ionization chamber [11].

The main goal of this experiment was to reduce the uncertainties of ^{239}Pu(n,γ) reaction cross section, providing a capture yield with an overall uncertainty 3% in the range from thermal energies to 10 keV. In order to achieve the required precision, we performed measurement of ^{239}Pu(n,γ) reaction at the n_TOF facility, using newly developed multi-section fission ionization chamber built at the University of Lodz in Poland. Like in the past in the previous n_TOF measurements, this apparatus was working in coincidence mode with the TAC. This detector of fission fragments improves some characteristics of the previously used experimental detection systems at the n_TOF facility [7,8,11]. For example, compared to previous detectors, it contains less material in the flux of neutrons as well as in surroundings of the samples, thereby reducing a background observed in the TAC. Moreover, it provides a better differentiation between alphas and fission fragments by their energy. This paper does not give results of the experiment performed at CERN, but describes the features and achievements of the multi-section Fission Ionization Chamber (mFIC).

2. The multi-section ionization chamber

Gamma rays from fission significantly contribute to the generation of background during measurement of ^{239}Pu(n,γ) reaction cross section, that is why fission must be tagged. Therefore, we used fission fragments (ff) detector in order to exclude fission-related γ-events registered by the TAC. We decided to develop a new multi-section fission ionization chamber (mFIC) which was used as the veto detector and placed in the centre of the TAC. To fulfil many requirements posed by the experimental conditions, multi-section ionization fission chamber should:

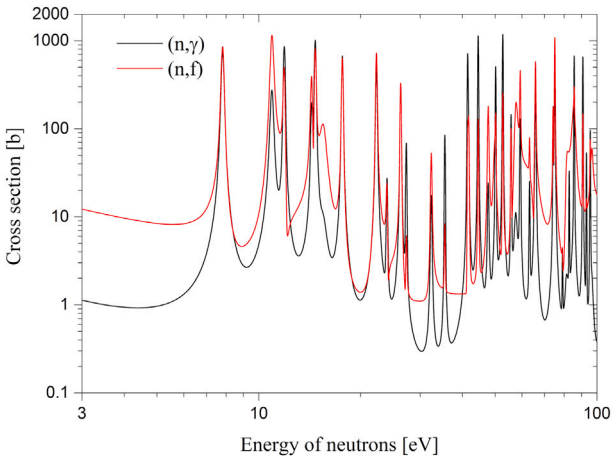

Fig. 1. The evaluated cross section of ^{239}Pu(n,γ) and (n,f) reactions at low neutron energies, from ENDF/B-VIII database [3].

(a) be fitted into a 10 cm radius sphere available inside the TAC detector;
(b) have as small as possible mass of construction materials intercepting the neutron beam, to minimize the gamma background in the TAC detector caused by the scattered neutrons;
(c) have active electronic elements outside the TAC crystal ball;
(d) assure assumed accuracy of the measurement and maximize the efficiency of detected fission fragments;
(e) separate α-particles from the fission fragments (ff) on the basis of their energy deposition in the gas;
(f) handle α-decay rates of order of $10^6 - 10^7$/s for assumed mass of ^{239}Pu 1 mg of each target, due to the half-life of ^{239}Pu (24 ky);
(g) achieve the best possible time resolution in optimum a few ns to obtain the best performance of the coincidence with the TAC and for reduction of pile-up of signals;
(h) minimize overcharging pulse called the gamma-flash, emitted while the proton bunch from PS interacts with the spallation target.

2.1. The characteristics of multi-section ionization fission chamber

To complete all the above requirements a new multi-section fission ionization chamber was proposed. Its schematic view is presented in Fig. 2, and corresponding picture of the chamber is shown in Fig. 3. The detector housing is on the left side with a connected cylindrical box containing preamplifiers on the right side. The neutron beam comes from the left side and runs along the entire length of the set-up along its symmetry axis. Neutrons move in the gas along the entire length of the detector between two thin mylar windows. The detector housing is placed at some distance from the preamplifier part to complete the requirements (a, b, c and h). The signal cables which connect the electrodes of the mFIC with the preamplifiers goes through the pipe shown in the middle, but special holder ensures that the cables do not cross the neutrons flux. High-voltage power supply cable and the plastic pipes for the gas flow are also visible in Fig. 3.

The dimension of the outer housing of the cylindrical chamber with 10 simple ionization chambers inside is 94 mm in diameter and 110 mm in length. These sizes/dimensions were strictly related to 10 cm radius of the sphere available in the centre of the TAC. The thickness of the wall of duralumin housing is 1 mm. To minimize the construction materials in the neutron beam, each of ten electrodes collecting the electric charge (anode) was made of 10 μm thick Al foil. The entrance and exit window of the detector was closed with 25 μm thick aluminized Kapton foil. This thickness of windows requires to use a pressure of the

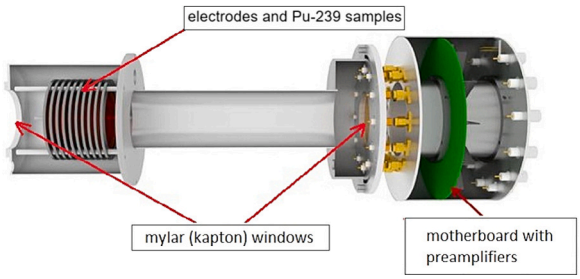

Fig. 2. Schematic view of the compact multi-section ionization chamber together with the cylindrical box for preamplifiers (on the right).

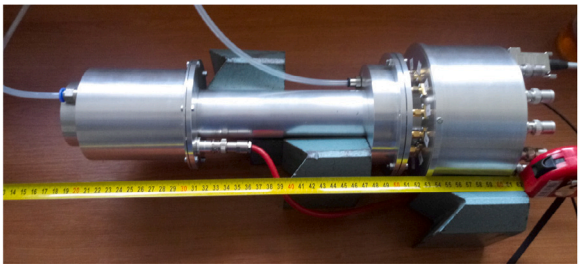

Fig. 3. Picture of the multi-section ionization chamber with connectors, two gas pipes and HV cable. The design of set-up ensures gas flow between the detector housing with electrodes and the part located in the immediate vicinity of the box with preamplifiers.

gas close to the atmospheric one. To achieve demanded statistics, 10 plutonium samples were used, each with a diameter of 20 mm deposited on 10 μm thick aluminium foil. Foils were stretched on duralumin rings with an internal diameter of 45 mm. More detailed information about the targets will be given in Sections 3 and 4.

The 90% Ar + 10% CF_4 gas mixture was used to fill the detector. This mixture is characterized by high drift velocity of electrons $V_D \sim$ 12 cm/μ in maximum [12], which, with the applied distance between the electrodes equals 4.5 mm, allows to obtain ∼40 ns of rise time for the observed pulses. In addition, this gas mixture allowed to minimize overload of the detector usually generated by recoil protons when fast neutrons interact with hydrogen nuclei. In our case, the absence of hydrogen atoms in the gas eliminated this effect, which affects the ability to record fission fragments in a wide range of neutron energies. The gas flow ensured the stability of the gas mixture composition during measurements and was regulated by means of a needle valve. The gas pressure was kept by means of the height of the oil column in the liquid manometer. This solution prevents oxygen from entering to the detector. Any admixture this gas causes a drastic loss of operating parameters of the ionization chambers. The gas outlet in an open continuous flow system was protected by a filter approved appropriately in advance by the dosimetry service.

2.2. Determination of distance between electrodes

The distance between the cathodes and anodes was selected based on simulations carried out using the SRIM software [13]. This distance of 4.5 mm between the electrodes was chosen as a compromise between two opposing characteristics of ionization chamber for a fixed electric field:

- the smaller the distance between the electrodes, the shorter the rise time of pulses,
- the greater the distance, the better the energy resolution of the chamber, since the higher energy of alpha particles and fission fragments will be deposited in the gas.

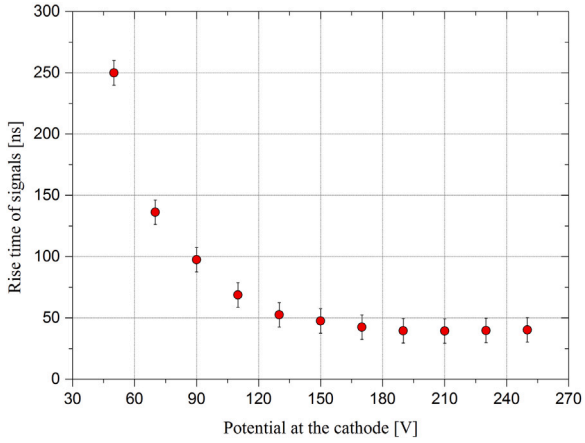

Fig. 4. Measured rise times of signals from fission fragments as a function of cathode voltage.

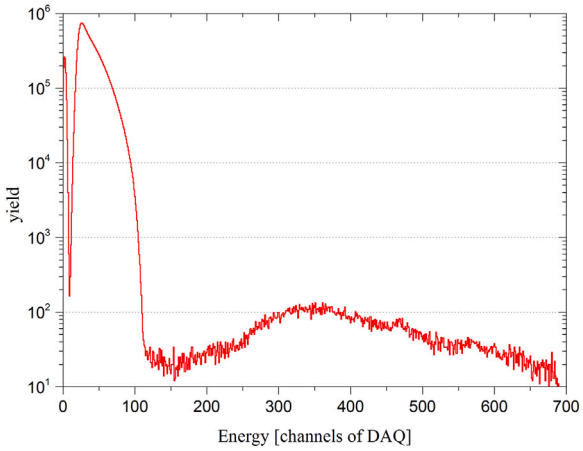

Fig. 5. Pulse-height spectrum of alphas and fission fragments from ^{235}U. The fission reaction was induced by neutrons from Pu-Be source. This measurement was performed without any high gamma background and the gamma-flash present at EAR1. The noise (up to channel ~10), alpha particles (between channel 10 and 110) and fission pulses (the broad spectrum from about channel 150) could be easily separated for all sections of the mFIC.

To perform the experiment with a required statistical accuracy and considering the available neutron beam intensity and the beam time, we have calculated the needed mass of ^{239}Pu. In order to provide an acceptable rate of alpha signals that could be processed by each sector of ionization chamber and an optimal thickness of the samples for fission fragment registration, 10 ionization chambers with ^{239}Pu samples were found to the appropriate solution. This, in turn, limited the maximum distance between the electrodes in the detector. The used gas mixture (Ar + CF_4) allowed to obtain the rise time for pulses from fission fragments of about 40 ns ($HV = -210$ V(470 V/cm)) for the distance between the electrodes of 4.5 mm, what is shown in Fig. 4. Our measurement confirmed the literature data, that the maximum drift velocity of electrons is $V_D \sim 12$ cm/μs for the used gas mixture at atmospheric pressure [12]. These simulations showed that a 4.5 mm distance between the electrodes gives good separation of signal amplitudes from alpha particles and fission fragments. The alpha particles from the Pu decay can deposit in the gas their total energy of 5.2 MeV on trajectories only very different from perpendicular to the target. Their ranges in the used gas mixture and normal pressure are about 36 mm. Contrary to this, the minimum energy that can be deposited by the fission fragments at the electrode spacing applied (4.5 mm) is greater than 20 MeV. For example, the fission fragments range is 17 mm for 50 MeV Cs and 25 mm for 100 MeV Cs. Therefore, the alpha particles and fission fragments can be separated in the pulse-height spectrum. The spectrum obtained during first tests of the mFIC were performed at University of Lodz with using Pu-Be neutron source and only availably ^{235}U sample is shown in Fig. 5.

2.3. The electronic pulse processing system

The signals from 10 independent section of the mFIC were amplified by the standard A1422H CAEN preamplifiers, located inside the cylindrical housing connected to the chamber extension. This construction was used to put the preamplifiers outside the TAC crystals. Such solution allowed to decrease the gamma-ray background generated by the interactions of scattered neutrons with material of preamplifiers. The 12 charge-sensitive preamplifiers (2 of them spare) implemented on a single in-line package (2 are spare) were placed inside cylindrical housing and soldered to the round motherboard with a hole inside it. This hole was specially designed to guarantee no interaction of neutron beam with the box of preamplifier. This used CAEN electronic module supports detectors up to 200 pF capacity and with sensitivity 45 mV/MeV (Si). These preamplifiers ensure about 5 ns minimal rise time of signals and can afford a very high count rate. The scheme of the round motherboard and a picture of the mounted preamplifiers is presented in Fig. 6. After amplification by a fast analogue amplifier, signals were sent to the digitizers.

Fig. 6. Scheme of the round motherboard, left panel. Photo of the interior of cylindrical housing with the preamplifiers, right panel.

Table 1
Atomic abundances of used Pu material determined by TIMS at JRC Geel.

Isotope	Amount fraction
$n(^{238}Pu)/n(Pu)$	<0.00002
$n(^{239}Pu)/n(Pu)$	0.9990259 (14)
$n(^{240}Pu)/n(Pu)$	0.0005818 (4)
$n(^{241}Pu)/n(Pu)$	0.0002501 (5)
$n(^{242}Pu)/n(Pu)$	0.0001288 (7)
$n(^{244}Pu)/n(Pu)$	<0.000002

3. Target preparation and characterization

The ^{239}Pu samples were prepared at the JRC Geel target preparation laboratory by molecular plating on an aluminium backing in isopropanol (C_3H_8O) using an in-house made polyacetal molecular plating cell with rotating Pt anode [14]. A mask on top of the backing incorporated in the molecular plating cell defined the diameter of the plutonium deposit. The Pu layers with a diameter of 20 mm consisted of deposited Pu material with some remaining isopropanol. As mentioned in Section 2.1 the backing was a 10 μm thick aluminium foil and it was stretched and glued on a duralumin ring with an internal diameter of 45 mm and an external diameter of 53.5 mm. The Pu base material was analysed for its atomic abundances by thermal ionization mass spectrometry (TIMS) at the JRC Geel nuclear chemistry and nuclear mass spectrometry laboratories and its composition is given in Table 1.

The ^{239}Pu alpha activities were determined by alpha-particle counting at a defined solid-angle and were calculated from the integrated count rate between 1 MeV and 6 MeV deposited alpha energy. In this

Table 2
Characteristics of the Pu targets prepared at JRC.

Sample position in the mFIC	Activity [MBq]	^{239}Pu mass [μg]	Areal density [μg/cm^2]
1	2.238 (7)	975 (3)	310.5 (10)
2	2.214 (3)	964.3 (13)	307.3 (4)
3	2.199 (3)	957.9 (12)	305.2 (4)
4	2.099 (3)	914.4 (12)	291.3 (4)
5	0.2862 (4)	124.65 (17)	39.72 (6)
6	1.935 (3)	843.0 (12)	268.6 (4)
7	2.186 (5)	952.3 (2)	303.4 (7)
8	2.110 (3)	919.0 (12)	292.8 (4)
9	2.094 (3)	911.9 (13)	290.5 (4)
10	2.253 (4)	981.1 (19)	312.6 (6)

energy region there are additional contributions due to the decay of such contaminations as ^{238}Pu, ^{240}Pu, ^{241}Pu, ^{242}Pu and ^{244}Pu as well to the decay of ^{241}Am. The contribution from the decay of Pu isotopes was derived from the atomic abundances of used Pu material determined by TIMS. The ingrowth and decay of ^{241}Am was derived from the beta decay of ^{241}Pu, the purification date, and the Am/^{239}Pu activity ratio determined by gamma spectrometry. The background was measured with a blank target. The solid angle was calculated according to the diameter of the deposit, the diaphragm in front of the detector and the distance between both. This calculation is based on numerical integration and its practical algorithm is described to calculate the solid angle for an axially symmetric set-up with one or more diaphragms, taking into account the true radial activity distribution of the source. The integration of the solid angle is done over the angular degrees of freedom in the spherical coordinate system. The description of this procedure could be found in the publication [15]. The intrinsic detection efficiency of the alpha-particle detector was assumed to equal 1.0. The ^{239}Pu masses were obtained from the measured alpha activities and the specific activity of ^{239}Pu = $2.2960(10) \cdot 10^3$ MBq/g. The ^{239}Pu areal densities were calculated from the ^{239}Pu masses and the diameter of the Pu deposit. The surface of these samples was uniform with an accuracy around 5% [14]. An overview of the ^{239}Pu alpha activity, mass and areal density of individual samples is given in Table 2. The ^{239}Pu alpha activities are calculated on the date of the α particle counting measurement. The quoted uncertainty is the combined uncertainty due to the counting statistics and a 0.12% random uncertainty component due to the reproducibility of the measurement conditions evaluated in Ref. [16]. For the total uncertainty of the ^{239}Pu alpha activity, the quoted uncertainty has to be combined with common uncertainty components: 1.30% due to the correction for the background, 0.35% due to the correction for the solid angle. The correction for the ^{238}Pu, ^{240}Pu, ^{241}Pu, ^{242}Pu, ^{244}Pu and ^{241}Am contributions can be neglected because it is very small, so the total combined uncertainty equals 1.35%.

4. Mounting of ^{239}Pu targets in the detector

The example one of mounted sample in the mFIC is easy seen in Fig. 7. A schematic diagram of the multi-section fission ionization chamber and a picture of its structure is presented in Fig. 8. The detailed characteristics of the targets used in the experiment at CERN is given in Table 2. Intensity of the emitted alpha particles from the ^{239}Pu decay is about $2 \cdot 10^6 \alpha/s$ for each section of mFIC with thicker samples. The lowest mass sample (position 5) was placed intentionally in the centre of the experimental set-up. The data obtained from this sample at almost one order of magnitude lower thickness will allow to determine influence of effect of anisotropy of emission gamma photons from fission fragments on registering efficiency by the TAC. This correction will be applied to the data from others sectors of the mFIC.

Considering the thickness of the used electrodes and the 3 mm distance between two anodes, alpha particles and fission fragments

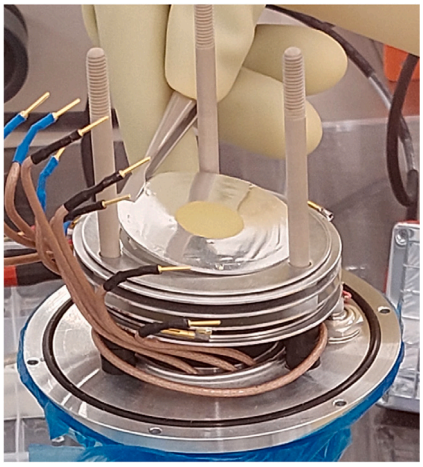

Fig. 7. Picture of the part of the detection system during the mounting process at the JRC in Geel. Plutonium material is the yellow region in the middle of aluminium target disk.

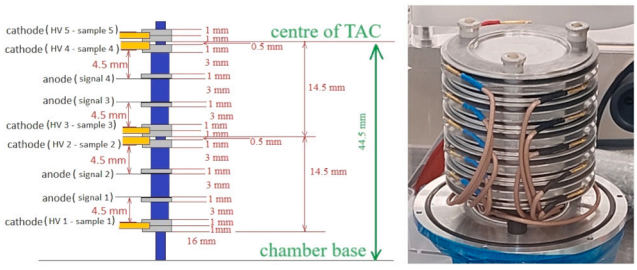

Fig. 8. Scheme of the fragment near one supporting rod of internal structure of the mFIC (left picture) and a photo of all 10 mounted sectors of ionization chamber (right picture). The rods and supporting structure made of non-conductive material are labelled in blue, whereas cathodes are marked in yellow. The positions of Pu samples on cathodes are shown as red lines. Only half of structure is shown to simplify the picture. The upper half is mirror reflection of the presented bottom part.

could penetrate the volume into the gas layer between individual sections of mFIC, but cannot reach the neighbouring section of the detector. The particles entering this area did not induce an electrical signal at the electrode of the next detector, because there was a zero difference of electric potential between the anodes.

5. Results from experiment at n_Tof facility, CERN

The n_TOF neutron time-of-flight facility is located at CERN [9,17,18], where neutrons are produced in spallation reactions, by impinging the lead target with a bunch of protons (7 ns rms) from Proton Synchrotron. The spallation target, that is cooled by gas nitrogen, is surrounded by borated and water layers to moderate the initially energetic neutrons, reduce γ - induced backgrounds. The moderated neutron spectrum is characterized by an almost isolethargic energy dependence and ranges from thermal energies to several GeV. The n_TOF facility consists of two experimental areas; Experimental Area 1 (EAR-1) is located at a distance of 185 m from the target, while Experimental Area 2 (EAR-2) for measurements requiring larger neutron flux is located at a distance of 20 m [9,17]. Recently, another measuring station called NEAR has been constructed very close to the spallation target for activation measurements [19]. Our experiment was performed at EAR-1, taking into account advantage of the excellent relative neutron energy resolution, which ranges from $3 \cdot 10^{-4}$ at 1 eV to $3 \cdot 10^{-3}$ at 100 keV [20].

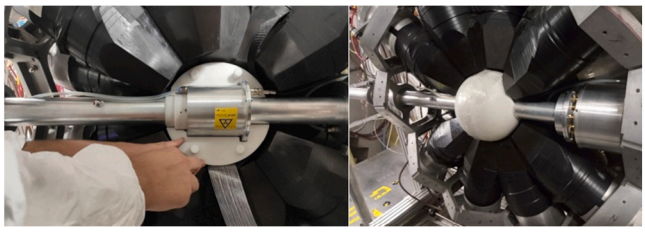

Fig. 9. The multi-section fission ionization chamber (mFIC) inside a spherical neutron absorber surrounded by half of BaF2 scintillators of the TAC.

5.1. The gamma-flash impulse and processing raw signals from detectors

To measure ^{239}Pu(n,γ) reaction cross section in tagging method, the mFIC was placed inside the TAC detector [7–9]. The TAC is a segmented 4π scintillator array consisting of 40 BaF_2 crystals 15 cm thick [7–9]. The crystals cover 95% of the solid angle, detecting cascade of γ-rays with high efficiency of typical total energies between 5 and 10 MeV and multiplicities that may range up to 6 or 8, depending on the investigated nucleus. To reduce the gamma background in BaF_2 crystals, traditionally used absorber of elastically scattered neutrons has been replaced with a special that allows the placement of mFIC. This 20 cm diameter absorber, made of polyethylene with lithium content, fills almost completely the space between the ionization chamber and the TAC crystals. It was designed at CIEMAT in Spain. The mFIC detector connected with neutron beam pipe in the centre of the TAC is shown in Fig. 9.

The presence of a pulse called the gamma-flash, arising from an interaction of 20 GeV proton bunch from PS with the spallation target, very often overloads the detectors and electronics at EAR1 and EAR2 [9]. This phenomenon represents an important challenge for detection, limiting the maximum neutron energy for which the detector can start registration of pulses. Therefore, this maximum neutron energy is the key parameter for each detector at n_TOF facility. The massive crystals of the TAC and the long slow light component (630 ns) contributed to significant pile-up effects of its signals, limiting the study of radiation capture in the ^{239}Pu(n,γ) reaction to neutron energy only up to several tens of keV. Due to the small amount of material in the neutron beam and the used additional electronic filters of low and high voltage supply in the preamplifiers, no pulse overloading mFIC was observed in the time spectrum. This difference is visible in Fig. 10 presenting the time spectra of raw pulses from the multi-section fission ionization chamber and the TAC detector simultaneously triggered. The TAC detector reaches equilibrium state after gamma flash signal in much longer time (~10 μs), what it could be noticed in Fig. 10.

Signals from the mFIC sections were processed with high performance digitizers, ADQ412 or ADQ414 [21], with 12 or 14 bit resolution respectively which are operated at 500 MSamples/s. The waveforms from digitizers were stored at CERN's computer centre. Later, these data are processed off-line to determine signal amplitudes and arrival time used in time-of-flight technique (TOF) for determination of incoming neutron energy. The dedicated Pulse Shape Analysis (PSA) routine special developed for this experiment are used for reconstructions of signal also from alphas and fission fragments detected by the mFIC.

5.2. Analysis of pulse-height spectra from mFIC

The spectrum of time differences between TAC and mFIC signals in the energy region close to the 0.3 eV resonance of ^{239}Pu is presented in Fig. 11. For the results presented in this paper we used 20 ns-wide coincidence window. The amplitude spectrum of alphas and fission fragments from ^{239}Pu, obtained using the mentioned earlier new dedicated PSA routine, is shown in Fig. 12. This spectrum allows easy separation of ff from alphas particles and the noise, This separation

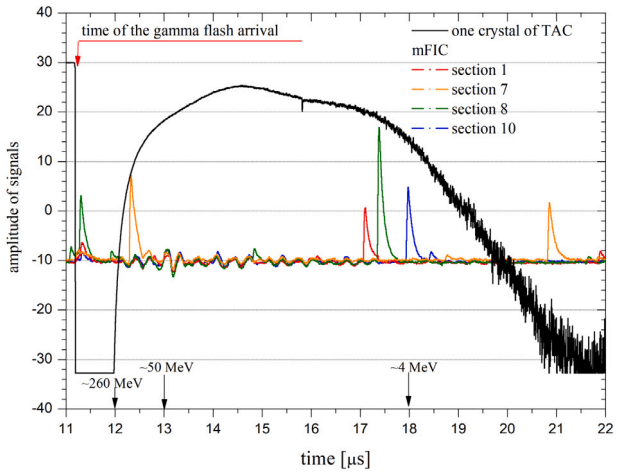

Fig. 10. Example of the signals from four mFIC sections and from one of the TAC crystal registered during the experiment at n_TOF. In the initial part of the signals from sectors of mFIC, small oscillations are seen, which have not got much impact on the discrimination of observed signals from fission fragments.

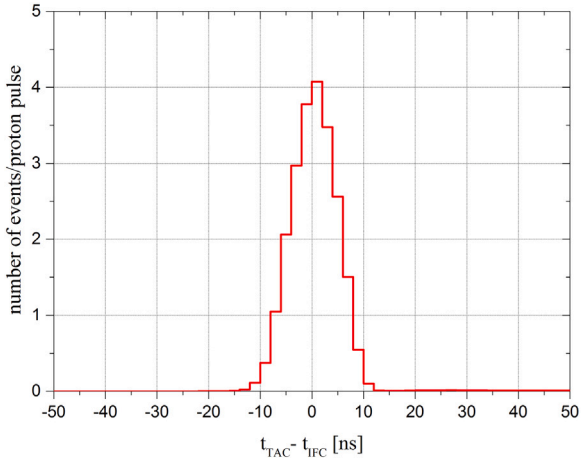

Fig. 11. The time coincidence spectrum between the TAC and the mFIC signals in the energy region close to the 0.3 eV resonance of ^{239}Pu.

is fully consistent with identification of ffs using coincidences with the TAC. Furthermore, this spectrum has got a similar structure to the spectrum shown in Fig. 4, which was obtained in conditions without the gamma-flash pulse. This discrimination between alpha and fission fragments was the one very important requirement in the performed measurement.

5.3. Time spectra of fission fragments and gammas

The efficiency of registration of the ffs by the one of the mFIC sections of with the thicker samples was determined experimentally based on coincidences with TAC, and it equals 0.90(5). The uncertainty of this value was estimated using the statistical and systematic error. The preliminary fission cross section from all the channels of the multi-section fission ionization chamber as function of neutron energy is presented in Fig. 13. It is worth to notice the very good agreement of our data with the ENDF/B-VIII data [3]. Data collected with mFIC are to be used mainly to identify and eliminate significant γ background contribution due to the fission in the ^{239}Pu(n,γ) reaction cross section measurement. However additionally, based on these new data, the ^{239}Pu fission cross section could be determined at least to $E_n = 5$ keV energy. Fig. 14 presents yields measured by the TAC and those from

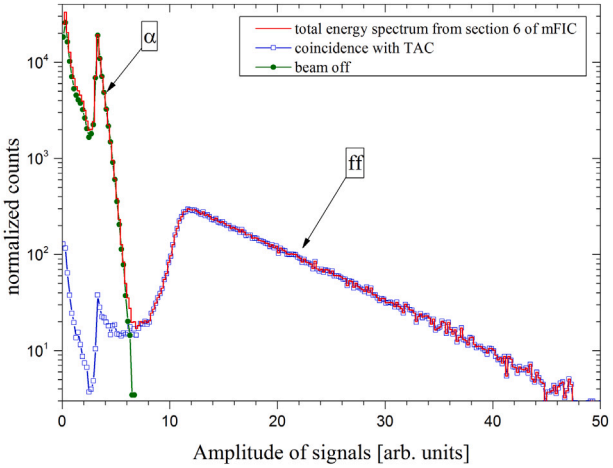

Fig. 12. Example of the pulse-height spectrum recorded by one of the mFIC section for neutrons energies from 0.1 eV to 10 keV. For comparison, the coincidence spectrum with signals from the TAC detector, and also spectrum registered without neutron beam are shown. The peak observed at amplitudes of 4 (blue squares) is artificial due to the threshold of the routine, so counts under this value are underestimated. It could be also noticed similar level of separation of alpha particles and fission fragments in pulse-height spectrum as in Fig. 5.

coincidence of TAC with the mFIC as a function of neutron energy. Only TAC events with 2.5–7 MeV deposited gamma-ray energy were considered here. The two spectra present the gamma events collected under condition of coincidence with mFIC and also total registered gamma spectrum (without coincidence). By comparison these spectra, it can be concluded that the new multi-section fission ionization chamber fulfilled its task in the measurement of radiative neutron capture reaction of ^{239}Pu with TAC at the n_TOF facility at CERN.

6. Conclusions

The multi-section fission ionization chamber was constructed and used in determination of the $^{239}\mathrm{Pu}(n,\gamma)$ reaction cross section as veto detector at the n_TOF facility at CERN. This paper presented description of the multi-section Fission Ionization Chamber (mFIC) layout and summarized the its most important properties. It is characterized by a high efficiency (~90%) for the thickness of the Pu samples that have been used, very good separation of alpha particles from fission fragments, short rise time of signals (40 ns) and resistance to the gamma flash signal appearing at the n_TOF facility. Results of the experiment performed at the n_TOF facility at CERN proof that this detector is very useful for the fission tagging technique applied for radiative neutron capture cross section measurements and we are going to publish soon the data for of the $^{239}\mathrm{Pu}(n,\gamma)$ reaction.

CRediT authorship contribution statement

J. Perkowski: Writing – original draft, Methodology, Conceptualization.

Declaration of competing interest

The authors declare the following financial interests/personal relationships which may be considered as potential competing interests: J. Perkowski reports financial support was provided by Narodowe Centrum Nauki (NCN). J. Andrzejewski reports financial support was provided by Ministry of Science and Higher Education of Poland. J. Perkowski, V. Alcayne, J. Andrzejewski, D. Cano-Ott, E. Mendoza, A. Sanchez-Caballero reports financial support was provided by UE

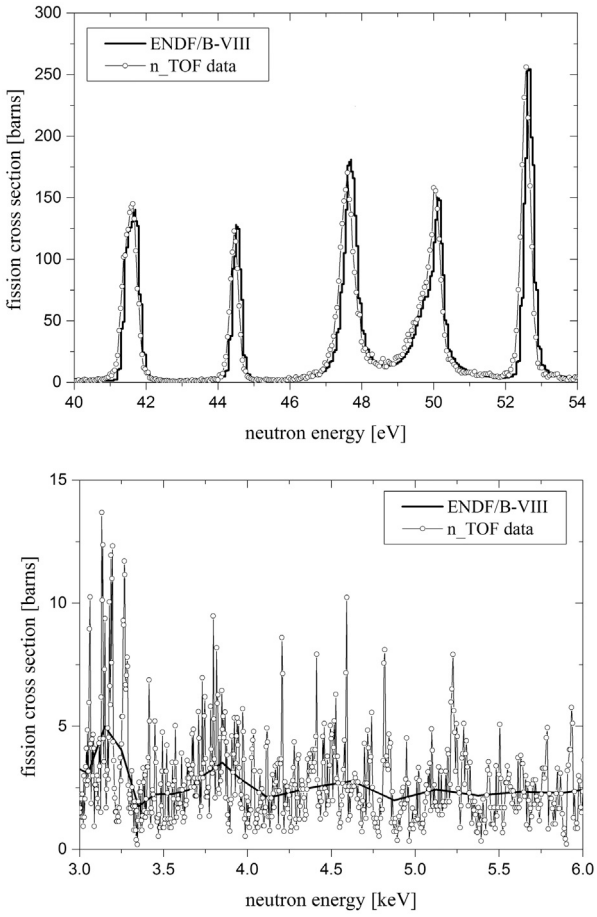

Fig. 13. The preliminary ^{239}Pu fission cross section data from all sections of mFIC as a function of neutron energy. A comparison between experimental n_TOF data and ENDF/B-VIII database at low energies with a very good separation of resonances (top) and at higher energies, where data for individual resonances are not available in evaluations (bottom).

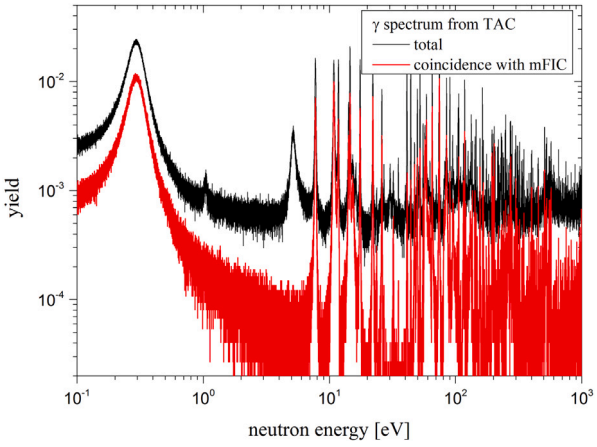

Fig. 14. The yield measured with the TAC detector and in coincidence with mFIC as a function of neutron energy. Only events with deposited gamma-ray energy sum between total sum energy between 2.5 and 7 MeV in the TAC and multiplicity higher than one were considered.

in the frame of the SANDA grant nr 847552. V. Alcayne, D. Cano-Ott, E. Mendoza, A. Sanchez-Caballero reports was provided by Spain Ministry of Science and Innovation. P. Zugec reports was provided

by Croatian Science Foundation project. G. Sibbens, D. Vanleeuw reports was provided by CHARPU project, Research Infrastructure Access Agreement. A. Gawlik-Ramiega reports financial support was provided by University of Lodz. If there are other authors, they declare that they have no known competing financial interests or personal relationships that could have appeared to influence the work reported in this paper.

Data availability

Data will be made available on request.

Acknowledgements

We acknowledge support of Narodowe Centrum Nauki (NCN), Poland (Grant No. UMO-2021/41/B/ST2/00326) and UE in the frame of the SANDA grant nr 847552 (Horizon 2020 project) and project of Ministry of Science and Higher Education of Poland nr 450734/PnH 2/2019 and Projekt Miedzynarodowy Wspolfinansowany Nr W93/H2019/Euratom/2019 (5099/H2020-Euratom/2020/2) and also University of Lodz under the grant (9/IDUB/MLOD/2021). This work was partially supported by PGC2018-096717- B-C21, and PID2022-142589OB-I00 funded by MCIN/AEI/10.13039/501100011033 and also by Croatian Science Foundation project IP-2022-10-3878. The experimental data used in this research were generated through access to the GELINA facility under the Framework for access to the Joint Research Centre physical Research Infrastructures of the European Commission (CHARPU project, Research Infrastructure Access Agreement N° 36225/2/2021-1-RD-EUFRAT-GELINA).

References

[1] G. Aliberti, et al., Impact of nuclear data uncertainties on transmutation of actinides in accelerator-driven assemblies, Nucl. Sci. Eng. 146 (2004) 13–50.
[2] G. Aliberti, et al., Nuclear data sensitivity, uncertainty and target accuracy assessment for future nuclear systems, Ann. Nucl. Energy 33 (2006) 700–733.
[3] N. Otuka, et al., Towards a more complete and accurate experimental nuclear reaction data library (EXFOR): International collaboration between nuclear reaction data centres (NRDC), Nucl. Data Sheets 120 (2014) 272–276.
[4] M. Salvatores, Uncertainty and target AccuracyAssessment for innovative systems using recent covariance data evaluations, Nucl. Sci. NEA/WPEC 26 (2008) 1–465.
[5] G. de Saussure, et al., Measurement of the neutron capture and fission cross-sections and of their ratio alpha for 233U, 235U and 239Pu, in: Proc. Conf. Nuclear Data, Microscopic Cross Sections, and Other Data Basic for Reactors, 1967, pp. 233–249.
[6] E. Dupont, et al., HPRL – international cooperation to identify and monitor priority nuclear data needs for nuclear applications, EPJ Web Conf. 239 (2020) 15005–15008.
[7] C. Guerrero, et al., Simultaneous measurement of neutron-induced capture and fission reactions at CERN, Eur. Phys. J. A 48 (2012) 29.
[8] M. Mastromarco, et al., High accuracy, high resolution 235U(n, f) cross section from n_TOF (CERN) from 18 meV to 10 keV, Eur. Phys. J. A 58 (2022) 147.
[9] F. Gunsing, et al., Nuclear data activities at the n_TOF facility at CERN, Eur. Phys. J. Plus 131 (2016) 371.
[10] J. Balibrea-Correa, et al., Measurement of the α ratio and (n,γ) cross section of 235U from 0.2 to 200 eV at n_TOF, Phys. Rev. C 102 (2020) 044615.
[11] M. Bacak, et al., A compact fission detector for fission-tagging neutron capture experiments with radioactive fissile isotopes, Nucl. Instrum. Methods Phys. Res. A 969 (2020) 163981.
[12] L.G. Christophorou, D.L. McCorkle, D.V. Maxey, J.G. Carter, Fast gas mixtures for gas-filled particle detectors, Nucl. Instrum. Methods Phys. Res. A 163 (1979) 141–149.
[13] J.F. Ziegler, J.P. Biersack, D.J. Marwick, G.A. Cuomo, W.A. Porter, S.A. Harrison, SRIM 2013 code, available from http://www.srim.org/.
[14] Goedele Sibbens, Alf Göök, David Lewis, André Moens, Stephan Oberstedt, David Vanleeuw, Ruud Wynants, Mariavittoria Zampella, Target preparation for neutron-induced reaction measurements, EPJ Web Conf. 229 (2020) 04003.
[15] S. Pommé, L. Johansson, G. Sibbens, B. Denecke, An algorithm for the solid angle calculation applied in alpha-particle counting, Nucl. Instrum. Methods Phys. Res. A 505 (2003) 286–289.
[16] R. Capote, et al., Unrecognized sources of uncertainties (USU) in experimental nuclear data, Nucl. Data Sheets 163 (2020) 191–227.
[17] Patronis, et al., Status report of the n_Tof facility after the 2nd CERN long shutdown period, EPJ Tech. Instrum. 10 (2023) 13.
[18] R. Esposito, et al., Design of the third-generation lead-based neutron spallation target for the neutron time-of-flight facility at CERN, Phys. Rev. Accel. Beams 24 (2021) 093001.
[19] M. Ferrari, et al., Design development and implementation of an irradiation station at the neutron time-of-flight facility at CERN, Phys. Rev. Accel. Beams 25 (2022) 103001.
[20] C. Guerrero, et al., Performance of the neutron time-of-flight facility n_TOF at CERN, Eur. Phys. J. A 49 (2013) 27.
[21] SP Devices, The SP devices website, 2019, URL https://www.spdevices.com.